Available online at www.sciencedirect.com
ScienceDirect
Ceramics International 35 (2009) 617–622
CERAMICS INTERNATIONAL
www.elsevier.com/locate/ceramint

Preparation of PZT discs for use in an acoustic wave sensor

M.I.S. Veríssimo [a], P.Q. Mantas [b], A.M.R. Senos [b], J.A.B.P. Oliveira [a], M.T.S.R. Gomes [a,*]

[a] Department of Chemistry/CESAM, University of Aveiro, 3810-193 Aveiro, Portugal
[b] Department of Ceramic and Glass Engineering/CICECO, University of Aveiro, 3810-193 Aveiro, Portugal

Received 20 November 2007; received in revised form 3 January 2008; accepted 18 January 2008
Available online 24 April 2008

Abstract

Ferroelectric ceramics based on lead zirconate titanate with Nb and Mn additives, for use in chemical sensing, have been prepared. The perovskite phase was produced by solid phase reaction of oxides/carbonates. Powders were shaped in the form of discs by uniaxial pressing, and sintered in a controlled atmosphere at several temperature and time conditions.

The microstructure of the sintered samples was observed in a scanning electronic microscope (SEM) and the grain size and density were shown to be dependent on the ceramic composition.

PZT ceramic discs showed strong radial vibration modes in the kHz range, which could be used for chemical sensing applications both in gaseous and liquid media. Sensitivity was found to be strongly dependent on the density of the ceramics.

Keywords: A. Powders: solid state reaction; C. Piezoelectric properties; D. PZT; E. Sensors

1. Introduction

Crystals of quartz are normally used in acoustic wave devices because they present an excellent stability of the resonant frequency, which allows the detection of changes in frequency as low as 0.1 Hz or at least 1 Hz in routine analyses. Although the crystals of quartz proved to be adequate in acoustic sensing devices [1,2], other piezoelectric materials are being seek for in order to lower costs and to get more flexibility on the final product. Barium titanate was the first material to be used in piezoelectric ceramic devices, but it has been substituted by the lead zirconate titanate (PZT) solid solutions since their discovery in 1954, when Jaffe et al. [3] reported unusual high piezoelectric properties of poled PZT ceramics with a chemical composition near the 50/50 (Zr/Ti) molar ratio. $Pb(Zr_xTi_{1-x})O_3$ solid solutions have shown large piezoelectric planar coupling coefficient (k_p), high dielectric permittivity and Curie temperatures $T_C > 230\ ^\circ C$ [4]. Furthermore, PZT are easier poled and easier to be sintered at lower temperatures than barium titanate.

A few attempts have been made to use PZT ceramics in mass sensors and promising results have been published for sensors in gaseous media, either using resonant piezo-layer sensors [5,6], or in SAW devices [7]. However, the use of this PZT ceramics as bulk acoustic wave sensors in liquid media has not been reported as the liquid seems to seriously damp the resonance signal [8,9]. The aim of this work was to manufacture PZT ceramic discs and to test them as chemical transducers in liquid media.

2. Experimental

2.1. Reagents

$PbCO_3$, TiO_2, ZrO_2, MnO_2 (all pro analysis) and PbO and Nb_2O_5 (99.9%) oxides were used as starting materials. A commercial PZT powder Piezokeramica 841 (APC International) was also used for comparison.

s-Butylamine (Merck 801540) and fructose (Panreac 14728) purissimum grade were used without any further purification. Nitrogen was Alphagaz grade from "Arlíquido".

2.2. Apparatus

In the mixing procedure, a Restch S1000 mill, set to a velocity of 30 rpm, was used.

Gold electrodes were deposited by sputtering using a SEM Coating Unit E5000.

* Corresponding author. Tel.: +351 234370722; fax: +351 234370084.
E-mail address: mtgomes@ua.pt (M.T.S.R. Gomes).

0272-8842/$34.00
doi:10.1016/j.ceramint.2008.01.016

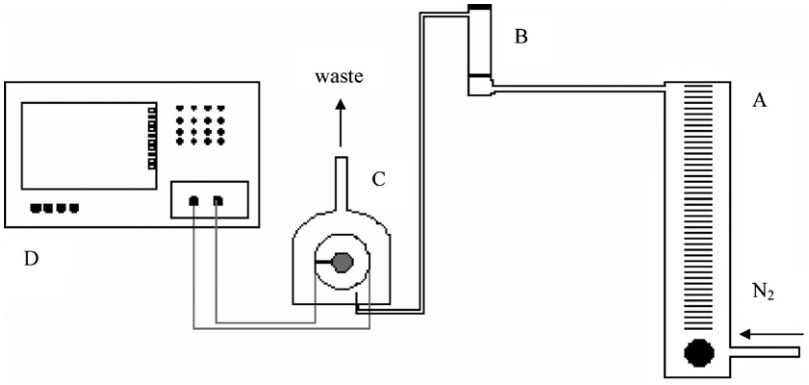

Fig. 1. Experimental layout for gaseous media: (A) flowmeter; (B) injection port; (C) cell and (D) Network/Spectrum/Impedance Analyser.

d_{33} (a piezoelectric constant relating the charge collected on the electrodes to the applied mechanical stress) was measured, at 120 Hz, with a Berlincourt Piezo d-Meter, previously calibrated.

Electric measurements were performed using the Impedance Analyser mode of a HP 4395A Network/Spectrum/Impedance Analyser. The analyser is equipped with a HP 43961 impedance Test Kit and the resonators were connected through a HP 16092A test Fixture.

Fig. 1 shows the experimental layout used for *s*-butylamine vapour detection. The ceramic discs were inserted into a cell and connected to the Network Analyser. A constant nitrogen flow of 30 mL min^{-1}, controlled by a flowmeter, carried the injected amine to the ceramic.

To perform measurements in liquid media, the ceramic discs were inserted in a special cell for liquids (ICM-International Crystal Manufacturing Co., Inc.). Fig. 2 shows the experimental layout. A constant nitrogen pressure of 10^4 Pa was maintained inside two reagent bottles. The pressure was controlled by a pressure regulator (OMNIFIT 3101) and is the driving force for the displacement of the liquid from the bottles into the cell. One of the bottles contained Milli-Q water and the other the sample. A three-way valve selects the fluid that goes into the sensor cell.

Measurements of the electric parameters were initially made with a frequency span that extended over the entire region of interest of the sensor (from 100 to 200 kHz). For analytical detection, the evolution of a particular frequency signal was followed, and the Network Analyser scanned 801 points around the frequency of interest with a 100 Hz bandwidth. Series frequency (f_s) was measured for vapour detection, while for liquids the frequency at minimum impedance (f_n) was measured, in accordance with previous work [10]. Eight scans were averaged for each measurement in liquid media, while for vapour single measurements were recorded. All impedance data presented in this work were obtained after calibration and test fixture compensation.

2.3. Procedure

2.3.1. Preparation of the ferroelectric ceramic discs

Ceramic samples were prepared by the conventional mixed oxide method [11–13]. TiO_2, ZrO_2, $PbCO_3$, PbO, MnO_2 and Nb_2O_5 were weighed according to the following compositions: $Pb(Zr_{0.530}Ti_{0.455}Nb_{0.015})O_3$, $Pb(Zr_{0.525}Ti_{0.465}Mn_{0.01})O_3$ and $Pb(Zr_{0.530}Ti_{0.470})O_3$.

Approximately 0.1 wt% of MnO_2 was added to the $Pb(Zr_{0.530}Ti_{0.455}Nb_{0.015})O_3$ composition, in order to increase the quality factor Q [14]. PbO was added in excess to compensate for PbO evaporation and to promote the densification [15].

Discs of ~2 cm diameter were obtained by uniaxially pressing at 187 MPa for 30 s. The usual sintering temperatures used to densify PZT samples prepared by the conventional process were around 1200 °C [16–18] and in this work 1150 and 1200 °C were chosen.

Fracture surfaces of sintered samples were observed by scanning electron microscopy (SEM).

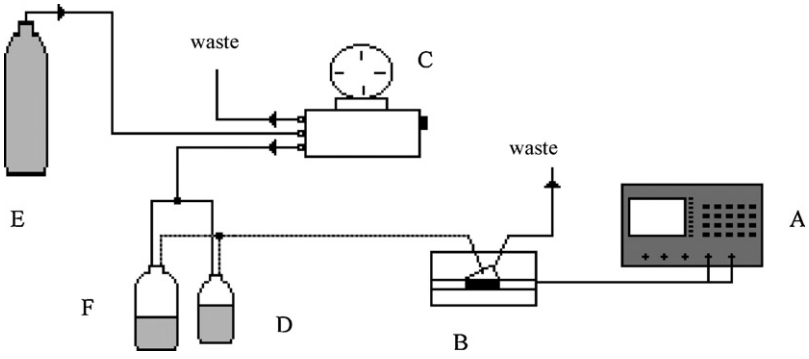

Fig. 2. Experimental layout for liquid media: (A) Network/Spectrum/Impedance Analyser; (B) cell; (C) pressure regulator; (D) sample bottle; (E) nitrogen and (F) water bottle.

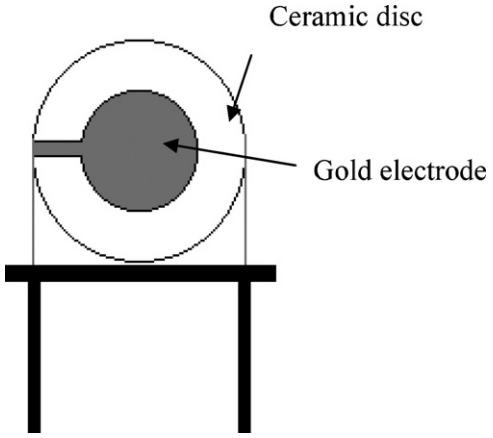

Fig. 3. Ceramic disc with gold electrodes mounted in a metal support.

After lapping and polishing the sintered bodies to a maximum thickness of 400 μm, silver electrodes were deposited on both sides. The samples were poled under a dc field of 40 kV cm^{-1} applied perpendicularly to the sample electrodes, in a silicone oil bath at 120 °C, for 30 min. After poling, silver electrodes were removed and new gold electrodes with 0.6 cm diameter were deposited, by sputtering. In order to be tested with the Impedance Analyser, the ceramic discs were bonded to a metal support in order to get the appropriate contacts. Fig. 3 shows a ceramic disc mounted by this process.

As piezoceramics are also commercially available, we included in this study a disc manufactured by the same methodology, prepared with a commercial PZT powder. Ferrari et al. [6] used a commercial PZT powder with low dielectric and mechanical losses, the Piezokeramica 841, and concluded that adding 20 wt% of PbO improved the electromechanical properties of the ceramic. Based on the good performance reported, a PZT sample was prepared with this Piezokeramica 841 powder, also with 20 wt% PbO, and was used for comparison with those ceramics prepared in the laboratory from PZT powders.

2.3.2. Frequency measurements in gaseous media

To test the performance of the ceramic discs for chemical sensing, an amine sample was injected through a septum located at the top of glass injection cell, shown in Fig. 1. A flow of nitrogen entering the bottom of the cell carries the amine vapour to the gold electrodes. The observed frequency decrease was monitored.

2.3.3. Frequency measurements in liquid media

Fig. 2 shows the experimental layout for measurements in liquid media. Milli-Q water was flowing through the cell housing the ceramic until constant frequency readings were obtained. Those readings were recorded and used as baseline. A solution of fructose was then allowed to flow over the ceramic disc and the difference between the frequency readings and baseline was computed. After each experiment, water was passed over the sensor until complete recover was achieved and baseline values have been restored. Eight scans were averaged for each measurement.

3. Results and discussion

The characteristics of the ceramic discs obtained by the described procedure are shown in Table 1. It can be observed that the values of the weight loss during sintering are related to the excess of PbO used, i.e., 0.8–1.7 wt% for 1 wt% excess PbO and 3.9–4.2 wt% for an excess of 5 wt% of PbO. Hence, the deviations from the stoichiometry are not significant and even in those cases where the weight loss is higher than the excess of PbO, leading to a deficiency in this element, the composition is still in the field of the PZT single phase and no precipitation of ZrO_2 is expected [16,19,20]. The excess of PbO leads to the formation of a PbO-rich liquid phase at temperatures below the value used for sintering, which enhances the densification process, but at higher temperatures and longer times this phase tends to disappear due to the preferential volatilisation of the PbO. The use of the theoretical density of PZT single phase, $\rho_t = 7.87$ g cm^{-3}, to obtain the relative densities, ρ, presented in Table 1 is therefore acceptable. This could not be done in the case of the sample prepared with the commercial powder due to the uncertainty on its chemical composition and to the high amount of excess PbO used. In this case, the relative density was not calculated.

Table 1
Characteristics of the ceramic discs

Composition		% PbO (w/w)	% MnO_2 (w/w)	Sintering conditions	Weight loss (%)	Density (g cm^{-3})	Relative density ρ (%)
1a	$Pb(Zr_{0.54}Ti_{0.47})O_3$	1	–	2 h/1150 °C	1.7	7.45	95
1b	$Pb(Zr_{0.54}Ti_{0.47})O_3$	1	–	2 h/1200 °C	1.6	7.69	98
2a	$Pb(Zr_{0.5247}Ti_{0.4653}Mn_{0.010})O_3$	1	–	2 h/1150 °C	0.8	7.24	92
2b	$Pb(Zr_{0.5247}Ti_{0.4653}Mn_{0.010})O_3$	1	–	8 h/1150 °C	1.4	7.32	93
2c	$Pb(Zr_{0.5247}Ti_{0.4653}Mn_{0.010})O_3$	1	–	2 h/1200 °C	1.3	7.36	93
2e	$Pb(Zr_{0.5247}Ti_{0.4653}Mn_{0.010})O_3$	5	–	8 h/1150 °C	–	7.66	96
2f	$Pb(Zr_{0.5247}Ti_{0.4653}Mn_{0.010})O_3$	5	–	2 h/1200 °C	4.2	7.40	94
3a	$Pb(Zr_{0.530}Ti_{0.455}Nb_{0.015})O_3$	1	0.1	2 h/1200 °C	1.0	7.32	93
3b	$Pb(Zr_{0.530}Ti_{0.455}Nb_{0.015})O_3$	5	0.1	2 h/1200 °C	3.9	7.59	96
4a	P841	20	–	2 h/930 °C	–	7.42	–

The results for the relative density (Table 1) show the following trends: (i) it increases when the sintering temperature increases (from 95 to 98% in the undoped case, from 92 to 93% in the Mn-doped samples); (ii) it increases with sintering time (92–93% from 2 to 8 h in the case of Mn-doped samples) and (iii) it increases with the amount of PbO excess (from 93 to 94%, in the case of 2 h sintering at 1200 °C of Mn-doped PZT, from 93 to 96% in the case of Nb-doped case). The addition of foreign elements, Mn or Nb, originates lower densities, but, as already seen, the density increases with the increase of the excess PbO amount. The enhancement of the densification with the addition of PbO was attributed to the formation of the PbO-rich liquid phase, as already mentioned, leading to a particle rearrangement and to an increase of the matter transport by a solution-precipitation process [17]. In order to evaluate the reproducibility of the manufacturing process, two extra ceramic disc samples with composition $Pb(Zr_{0.5300}Ti_{0.4550}Nb_{0.0150})O_3$, 5 wt% PbO excess and sintered for 2 h at 1200 °C have been produced. Densities of the three discs did not differ more than 1%.

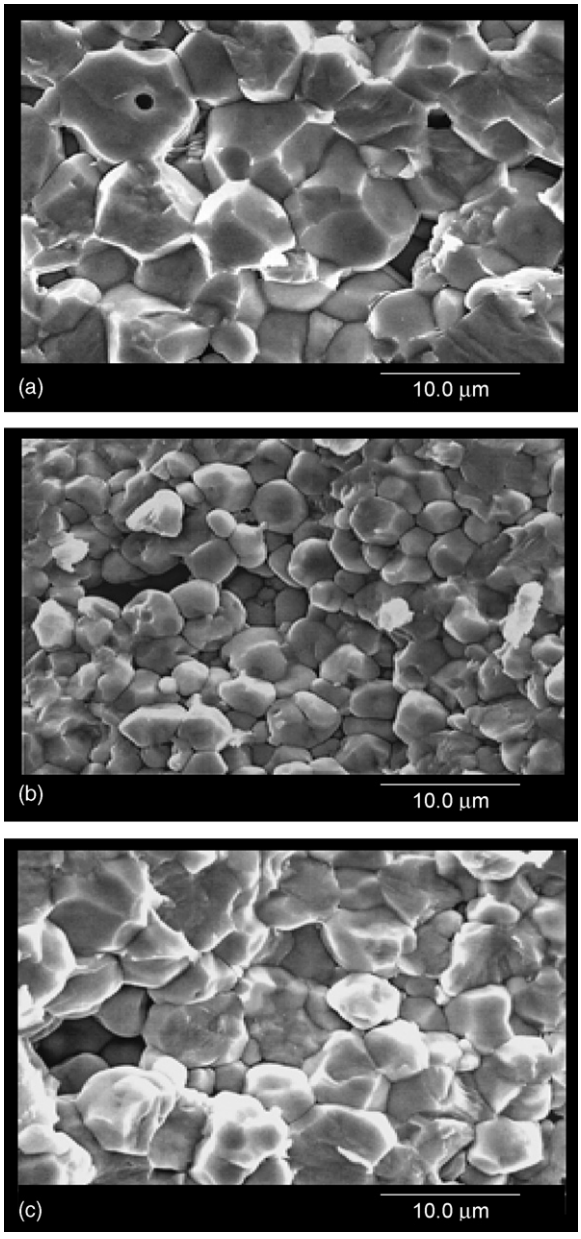

Fig. 4. Scanning electron micrographs of fracture surfaces of samples sintered 2 h at 1200 °C: (a) PZT, 1 wt% excess PbO, (b) Mn–PZT, 5 wt% excess of PbO, (c) Nb–Mn–PZT, 5 wt% excess PbO.

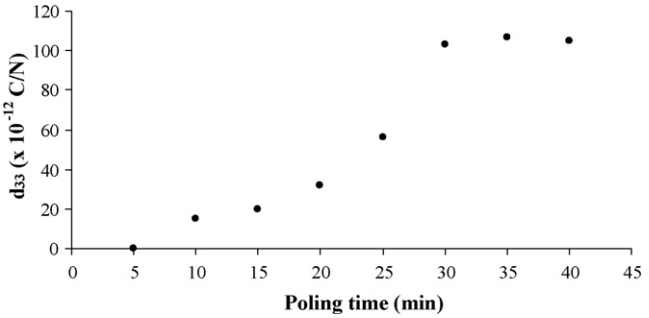

Fig. 5. Variation of the piezoelectric coefficient d_{33} with the poling time for ceramic 3b.

The microstructures presented in Fig. 4 do not show any evidence of the presence of second phases, namely particles of free zirconia, in agreement with the results of the weight loss previously discussed. The presence of a liquid phase is not clear, although its existence as thin films between the grains cannot be ruled out. The observed weight losses due to the volatilisation of PbO at the sintering temperatures lead to a strong reduction of the amount of the liquid phase previously formed and, therefore, it is difficult to detect its presence in the actual experimental conditions. Evidences of the existence of the thin film between the grains needed a more careful microscopic observation, namely by TEM.

Comparing Fig. 4(a) with Fig. 4(b) and (c), it can be observed that doped PZT samples show a smaller average grain size than that of the undoped ones. The reduction of the grain size by the presence of dopants, like Nb, is commonly observed in PZT and in other systems, even when solid solutions are created [21,22]. Although the excess of PbO used in the doped samples of Fig. 4(b) and (c) is higher than that of Fig. 4(a), which would lead to an increase of the grain growth rate [17], the dopant exerts an efficient pinning of the grain boundary movement, thereby decreasing the grain growth.

Discs were poled by the application of a dc field of 40 kV cm^{-1} and Fig. 5 shows the evolution of d_{33} coefficient with the poling time. From this figure, it can be seen that d_{33} increases with poling time up to 30 min, after which a much slower increase is observed. Therefore, all discs were poled for 30 min. Table 2 shows the electric and piezoelectric parameters

Table 2
Electric parameters of some of the ceramic discs

Discs	R_1 (Ω)	L_1 (mH)	C_1 (pF)	C_0 (nF)	k_p	Q_m	d_{33} ($\times 10^{-12}$ C/N)
1a	13.4	0.68	1706	12.9	0.40	63	110
2b	23.9	2.47	478.9	7.77	0.34	47	101
2c	34.7	2.86	620.1	8.98	0.36	90	132
3a	31.6	2.17	560.4	8.51	0.39	121	132
3b	20.1	1.54	792.4	13.4	0.43	135	105
4a	112	0.48	3658	9.30	–	7	90

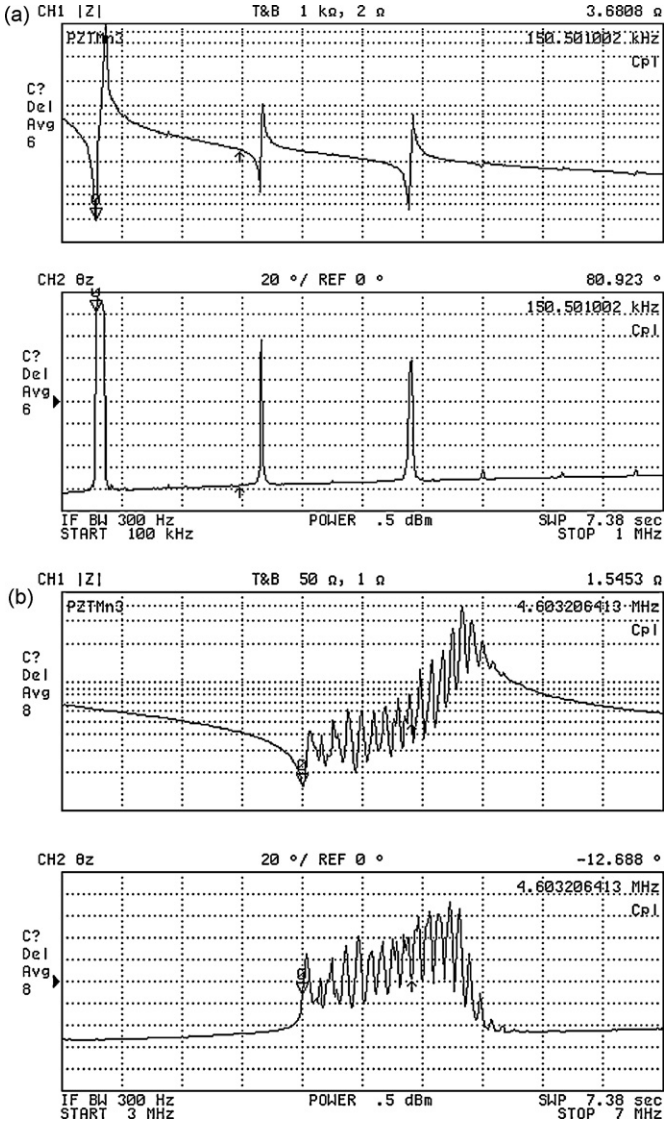

Fig. 6. Impedance modulus and phase vs. frequency for a disc of Nb–Mn–PZT in the kHz range (a) and in the MHz range (b).

of the ceramic discs for all the compositions measured after this poling procedure.

Fig. 6 shows a plot of the impedance and the phase vs. frequency for the piezoelectric ceramic 3b, in the kHz range (a) and in the MHz range (b). It can be observed in Fig. 6b that the ceramic disc in the MHz range shows many spurious vibrational modes. Therefore, the kHz range signals were chosen to be monitored in the experiments. This is the frequency range where the planar (radial) vibration mode operates (Fig. 6a) [23].

The frequency at minimum impedance (f_n) was measured and the parameters of the Butterworth–Van Dyke (BVD) equivalent electrical circuit [24] were calculated by the Network Analyser. Q was calculated using the inductance (L_1) and the resistance (R_1) values, through the following equation:

$$Q = 2\pi f_n \left(\frac{L_1}{R_1}\right) \quad (1)$$

Table 3
Frequency shifts observed for different amounts of *s*-butylamine, for several ceramic discs

Ceramic disc	Density (g cm^{-3})	Δf_s(30 μL) (Hz)	Δf_s(80 μL) (Hz)
1a	7.45	62	104
2b	7.32	16	48
2c	7.36	30	97
3a	7.32	29	95
3b	7.59	56	119
4a	7.42	56	99

In spite of the modest values for d_{33} and Q, the first signal in Fig. 6a was strong enough to expect the ceramic disc to work as a piezoelectric chemical sensor. After the insertion of each ceramic disc into the glass cell, shown in Fig. 1, 30 and 80 μL of *s*-butylamine were injected into the nitrogen stream that reach the ceramic disc and the series frequency shifts were registered. These shifts are shown in Table 3.

It is known that liquid samples can cause a severe damping in the sensor output. Fig. 7 shows the effect of water and a fructose solution on the impedance magnitude and phase of a disc of Nb–Mn–PZT. It is possible to observe the expected broadening and the decreasing of the intensity of the resonance peaks, although signals remain well defined and strong enough to allow analytical measurements. Table 4 shows the decrease of the frequency at minimum impedance obtained with aqueous solutions of fructose.

From Tables 3 and 4, it can be observed that all the ceramic discs, including those prepared with the commercial powder 841, can be used as mass sensors. However, the highest values for the frequency shifts, Δf, were found for the ceramic samples 1a and 3b, those which show the highest values for the relative density, $d \geq 95\%$. The signals obtained with these samples were just slightly higher than those obtained with the disc prepared from the commercial powder, used for comparison. Despite the effects of the composition and of the grain size, which are not well discernible in this work, the attainment of density values higher than 95% seems to be the relevant parameter to obtain a high sensitivity. It is known that the reduction of porosity implies an increase in the dielectric

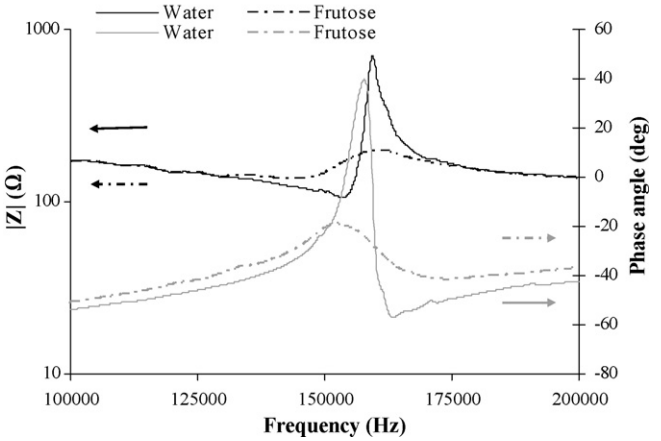

Fig. 7. Impedance and phase angle vs. frequency for a ceramic disc in contact with Milli-Q water and fructose solution.

Table 4
Shifts of the frequency at minimum impedance (f_n) observed for two solutions of fructose

Ceramic disc	Density (g cm^{-3})	5% (w/w) fructose Δf_n (Hz)	30% (w/w) fructose Δf_n (Hz)
1a	7.45	142	599
2b	7.32	56	205
2c	7.36	78	369
3a	7.32	82	361
3b	7.59	196	692
4a	7.42	139	590

permittivity, in the remnant polarisation and in the electromechanical factor and this is critical when changing from open to close porosity, a fact that normally occurs between 90 and 95% of relative density [25]. However, the good sensitivity values of the samples here prepared may also be attributed to the absence of crystalline second phases and to a presumable very low content of the PbO-rich amorphous phase. C_0 is the only parameter of the equivalent electric circuit directly related with the permittivity, and as it can be observed from Table 2, it generally increases with the increasing of density, just as expected.

4. Conclusion

All the ceramic discs manufactured, regardless of composition and sintering conditions, showed sensitivity to chemicals and frequency stability, which allowed their use as chemical sensors. Even in liquid phase good electrical signals have been obtained and sensitivity of the ceramics to fructose concentration evidenciates their aptitude for chemical sensing in liquid media.

The high sensitivity to *s*-butylamine, and fructose on aqueous solution is strongly dependent of the attainment of density values higher than 95% of the ceramic samples. The absence of crystalline second phases, other than PZT and the low content of PbO-rich amorphous phase also contribute to achieve a good performance of this material in a piezoelectric response.

Acknowledgments

The authors wish to thank the University of Aveiro for the financial support to the project. One of the authors, M.I.S. Veríssimo wishes to thank the Portuguese Science and Technology Foundation (FCT) for the scholarship PRAXIS XXI/BD/18279/98.

References

[1] M.T.S.R. Gomes, M.I.S. Veríssimo, J.A.B.P. Oliveira, New method for monitoring the contamination of glycerol with diethylene glycol, J. Pharm. Pharmacol. 51 (1999) 233–236.
[2] M.T.S.R. Gomes, K. Tavares, J.A.B.P. Oliveira, The quantification of potassium using a quartz crystal microbalance, Analyst 125 (2000) 1983–1986.
[3] B. Jaffe, R.S. Roth, S. Marzullo, Piezoelectric properties of lead zirconate–lead titanate solid-solution ceramics, J. Appl. Phys. 25 (1954) 809–810.
[4] G.H. Haertling, Ferroelectric ceramics: history and technology, J. Am. Ceram. Soc. 82 (1999) 797–818.
[5] M. Ferrari, V. Ferrari, D. Marioli, A. Taroni, M. Suman, E. Dalcanale, Cavitand-coated PZT resonant piezo-layer sensor: properties, structure and comparison with QCM sensors at different temperatures under exposure to organic vapors, Sens. Actuator B 103 (2004) 240–246.
[6] V. Ferrari, D. Marioli, A. Taroni, Thick-film resonant piezo-layers as new gravimetric sensors, Meas. Sci. Technol. 8 (1997) 42–48.
[7] S.-Y. Chua, T.-Y. Chen, I.-T. Tsai, W. Water, Doping effects of Nb additives on the piezoelectric and dielectric properties of PZT ceramics and its application on SAW device, Sens. Actuator A 113 (2004) 198–200.
[8] M. Yang, M. Thompson, Multiple chemical information from the thickness shear mode acoustic wave sensor in the liquid phase, Anal. Chem. 65 (1993) 1158–1168.
[9] C. Behling, R. Lucklum, P. Hauptmann, Response of quartz-crystal resonators to gas and liquid analyte exposure, Sens. Actuator A 68 (1998) 388–398.
[10] M.T.S.R. Gomes, M.I.S. Veríssimo, J.A.B.P. Oliveira, Analytical advantages of monitoring a particular characteristic frequency in a thickness shear mode acoustic wave sensor, Sens. Actuator B 78 (2001) 331–336.
[11] Y. Matsuo, H. Sasaki, Formation of lead zirconate titanate solid solutions, J. Am. Ceram. Soc. 48 (1965) 289–291.
[12] M.R. Soares, A.M.R. Senos, P.Q. Mantas, Phase coexistence in PZT ceramics, J. Eur. Ceram. Soc. 19 (1999) 1865–1871.
[13] M.R. Soares, A.M.R. Senos, P.Q. Mantas, Phase coexistence region and dielectric properties of PZT ceramics, J. Eur. Ceram. Soc. 20 (2000) 321–334.
[14] A.P. Barranco, A.H. Tera, L. Banos, J.G. Mendonza, Modified lead titanate zirconate system: preparation techniques and properties, J. Mater. Sci. Lett. 17 (1998) 1033–1035.
[15] M. Hammer, M.J. Hoffmann, Sintering model for mixed-oxide-derived. Lead zirconate titanate ceramics, J. Am. Ceram. Soc. 18 (1998) 3277–3284.
[16] A.I. Kingon, J.B. Clark, Sintering of PZT ceramics. I. Atmosphere control, J. Am. Ceram. Soc. 66 (1983) 253–256.
[17] A.I. Kingon, J.B. Clark, Sintering of PZT ceramics. II. Effect of PbO content on densification kinetics, J. Am. Ceram. Soc. 66 (1983) 256–260.
[18] G.S. Snow, Fabrication of transparent electrooptic PLZT ceramics by atmosphere sintering, J. Am. Ceram. Soc. 56 (1973) 91–96.
[19] T. Ikeda, Studies on (Ba–Pb)(Ti–Zr)O_3 system, J. Phys. Soc. Jpn. 14 (1959) 168–174.
[20] S. Fushimi, T. Ikeda, Phase equilibrium in the system PbO–TiO_2–ZrO_2, J. Am. Ceram. Soc. 50 (1967) 129–132.
[21] S. Cheng, S. Fu, C. Wei, Low-temperature sintering of PZT ceramics, Ceram. Int. 13 (1987) 223–231.
[22] R.J. Brook, in: F.F.Y. Wang (Ed.), Ceramic Fabrication Processes, Treatise on Materials Science and Technology, vol. 9, Academic Press, New York, 1976.
[23] Murata Manufacturing Co. Ltd., Piezoelectric ceramic sensors at http://www.murata.com/catalog/p19e.pdf.
[24] M. Yang, M. Thompson, Acoustic network analysis and equivalent circuit simulation of the thickness-shear mode acoustic wave sensor in the liquid phase, Anal. Chim. Acta 282 (1993) 505–515.
[25] L. Wu, C.-C. Wei, T.S. Lou, H.-C. Liu, Piezoelectric properties of modified PZT ceramics, J. Phys. C: Solid State Phys. 16 (1983) 2813–2822.